PUBLISHED VERSION

D.C. Whitea, M.M. Lewisa, G. Greenb, Travis B. Gotchc

A generalizable NDVI-based wetland delineation indicator for remote monitoring of groundwater flows in the Australian Great Artesian Basin

http://hdl.handle.net/2440/102223

A generalizable NDVI-based wetland delineation indicator for remote monitoring of groundwater flows in the Australian Great Artesian Basin

Davina C. White [a,*], Megan M. Lewis [a], Graham Green [b], Travis B. Gotch [c]

[a] School of Earth and Environmental Sciences, The University of Adelaide, Adelaide 5064, Australia
[b] Science, Monitoring and Knowledge, Department of Environment, Water and Natural Resources, South Australian Government, Adelaide 5001, Australia
[c] South Australia Arid Lands Region, Department of Environment, Water and Natural Resources, South Australian Government, Roxby Downs 5725, Australia

ABSTRACT

Improved understanding of the relationship between groundwater outflows from Australian Great Artesian Basin (GAB) springs and the extent of wetlands they support is urgently needed given projected increasing impacts of land use and groundwater extractions for mining operations within the region. This paper demonstrates the use of wetland area derived from analysis of high-resolution satellite imagery as an indicator of groundwater flow from springs in the GAB. The method developed was tested on three spring groups in South Australia, encompassing a diversity of spring forms, spatial extents, geomorphic and hydrogeological settings. The Normalised Difference Vegetation Index (NDVI) was computed from QuickBird and WorldView-2 satellite imagery captured to coincide with ground-based vegetation cover and spring discharge measurements. Significant linear relationships were established between image NDVI and ground-based vegetation cover, and from these relationships NDVI thresholds were determined to delineate GAB-fed wetlands from surrounding dryland vegetation. There were strong linear relationships between NDVI-derived wetland areas and spring flow rate measurements for selected springs ($R^2 = 0.92$ to 0.99). Although there were some differences in this relationship for the three sites, they were not statistically significant. This research demonstrates a relationship between surface flow rate and wetland area that is transferable to a range of GAB springs, which vary in spatial scale, outflow rates, surface form, geomorphic setting and vegetation composition. The technique provides an objective, quantitative and accurate means of documenting the distribution and extent of spring-fed wetlands: a relatively consistent NDVI threshold can be used to differentiate wetland from dryland vegetation and spring flow rates can be determined from image-derived wetland extents. This approach provides natural resource managers with an indicator of spring wetland response that can be used to monitor the impacts of land use, groundwater extractions and climate change over time for the GAB and potentially other aquifers worldwide.

© 2015 The Authors. Published by Elsevier Ltd. This is an open access article under the CC BY-NC-ND license (http://creativecommons.org/licenses/by-nc-nd/4.0/).

1. Introduction

The Great Artesian Basin (GAB) is one of the world's largest groundwater aquifers underlying approximately 1.76 million km² of the Australian continent (Habermehl, 1980) and containing an estimated 64,900,000 GL of water (Gotch et al., 2006). Along its western margin in northern South Australia the GAB supports a considerable number of wetlands fed by artesian springs, bores and surface waterholes (Fig. 1). The focus of this paper is the GAB springs, also known as mound springs, which have been ecologically important features in the landscape for around 750,000 thousand years (Gotch, 2013; Love et al., 2013). The stability and consistency of groundwater discharge from the GAB has been a primary determinant of the ecological significance of the springs (Gotch, 2013; Love et al., 2013). These distinctive permanent freshwater ecosystems are the result of natural groundwater discharge from the Cretaceous J Aquifer which is an unconfined to confined artesian aquifer, comprising of the Algebuckina Sandstone, Cadnaowie Formation and their lateral equivalents (Keppel et al., 2013a). The J Aquifer reaches the surface *via* fault-associated fractures in the overlying Bulldog Shale and Rumbalara Shale aquitards, which can reach a thickness in excess of 1000 m (Love et al., 2013).

* Corresponding author: Tel.: +61 0 8 313 8112.
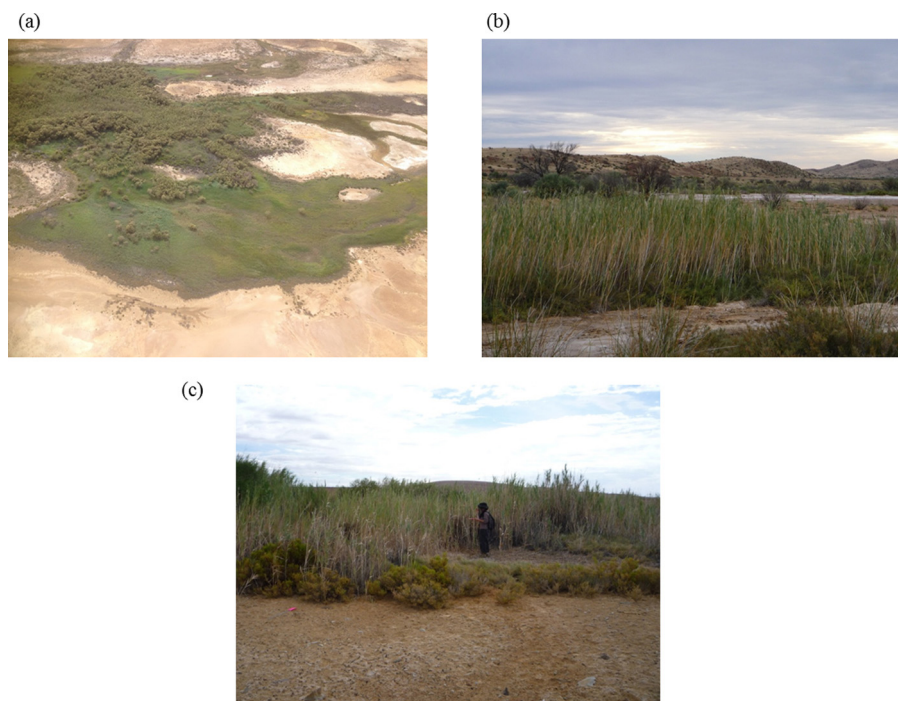*E-mail address:* davina.white@adelaide.edu.au (D.C. White).

Fig. 1. Nature of spring formations at: (a) Dalhousie Spring Complex (oblique aerial photo); (b) Freeling Spring Group (ground photo); and (c) Hermit Hill Spring Group (ground photo).

The springs were identified as important permanent sources of water by indigenous Australians thousands of years ago (Ah Chee, 2002). Since European settlement in 1878 the springs have provided a lifeline within the Australian arid zone, supporting a significant pastoral industry (Cox and Barron, 1998; Love et al., 2013). As a result of their environmental significance the springs have been protected since 1989 by the Australian Government under the Environment Protection and Biodiversity Conservation Act (Department of Sustainability, 2011). Attention to the sustainability of the springs has increased considerably in recent times due to current and projected groundwater extractions for mining operations. Therefore, there is an urgent need to develop effective and reliable tools to document and monitor flows from the GAB springs (White and Lewis, 2011).

Previous mapping and monitoring of the discharge and associated wetlands of GAB springs has been limited to a few studies, which have been fieldwork intensive. Williams and Holmes (1978) were the first to publish a technique to estimate the discharge from springs at Dalhousie Spring Complex (DSC) using aerial photography with current meter and bucket and stop-watch measurements of flow rates. Holmes et al. (1981) extended this study to include several quite contrasting springs within South Australia using a similar approach. BHP Billiton (2013a,b) developed a method to monitor changes in spring wetland extent for a selection of springs using classified aerial photography, but have not directly related this to spring flows (BHP Billiton, 2013a). These approaches are site-specific, time consuming and limited in their ability to discriminate spring wetlands from surrounding dryland vegetation (White and Lewis, 2011). More recently, advanced remote sensing techniques have been developed to quantitatively map and monitor GAB spring discharge (Lewis et al., 2013). The research revealed a strong direct relationship between spring discharge rate and the satellite image-derived wetland area from eight springs at DSC, confirming that wetland area can be used as an indicator of spring flow (White and Lewis, 2011). This method shows great potential as a remote monitoring tool for these spatially disparate and isolated wetlands. However, the transferability of the method to a wider range of springs with differing spatial extent, surface expressions and landscape settings has not yet been tested.

It is the intention of this paper to develop a remote monitoring tool of wetland vegetation extent that is less reliant on ground-based calibration, repeatable and consistent over space and time. A specific objective is to determine if the strong direct relationship between spring discharge rate and wetland vegetation extent, as demonstrated for Dalhousie by White and Lewis (2011), can be extended to additional contrasting spring groups. This will be particularly valuable for providing an objective, quantitative, repeatable method from which projected increased groundwater and land use impacts from mining operations in the GAB can be effectively monitored and managed. It will lead to improved understanding of the interaction between mining impacts, spring management practices and natural processes, including climate change, on these unique wetland ecosystems.

2. Materials and methods

2.1. Study area

GAB springs are defined as surface outlets where artesian water discharges from underlying confined aquifers *via* geological conduits. Recent research has improved our understanding of mound spring structures, their evolution and formation (Keppel et al., 2011, 2013b). Keppel et al. (2011) describe the springs of the Lake Eyre South region as having a pool in the vicinity of the discharge vent with a surrounding mound barrage structure composed of carbonate precipitated from the spring waters, combined with local or transported sand and clays (Clarke et al., 2007). Water then flows into an often densely vegetated delta-shaped fan or spring tail where carbonate precipitation is most active (Keppel et al., 2011). The formation of spring mounds is spatially dynamic, as during the lifetime of a spring the zone of active carbonate deposition may shift from near the vent to the tail delta (Keppel et al., 2011, 2013b). The vegetation surrounding spring vents, spring tails and the intervening country is varied in plant species composition and spatial
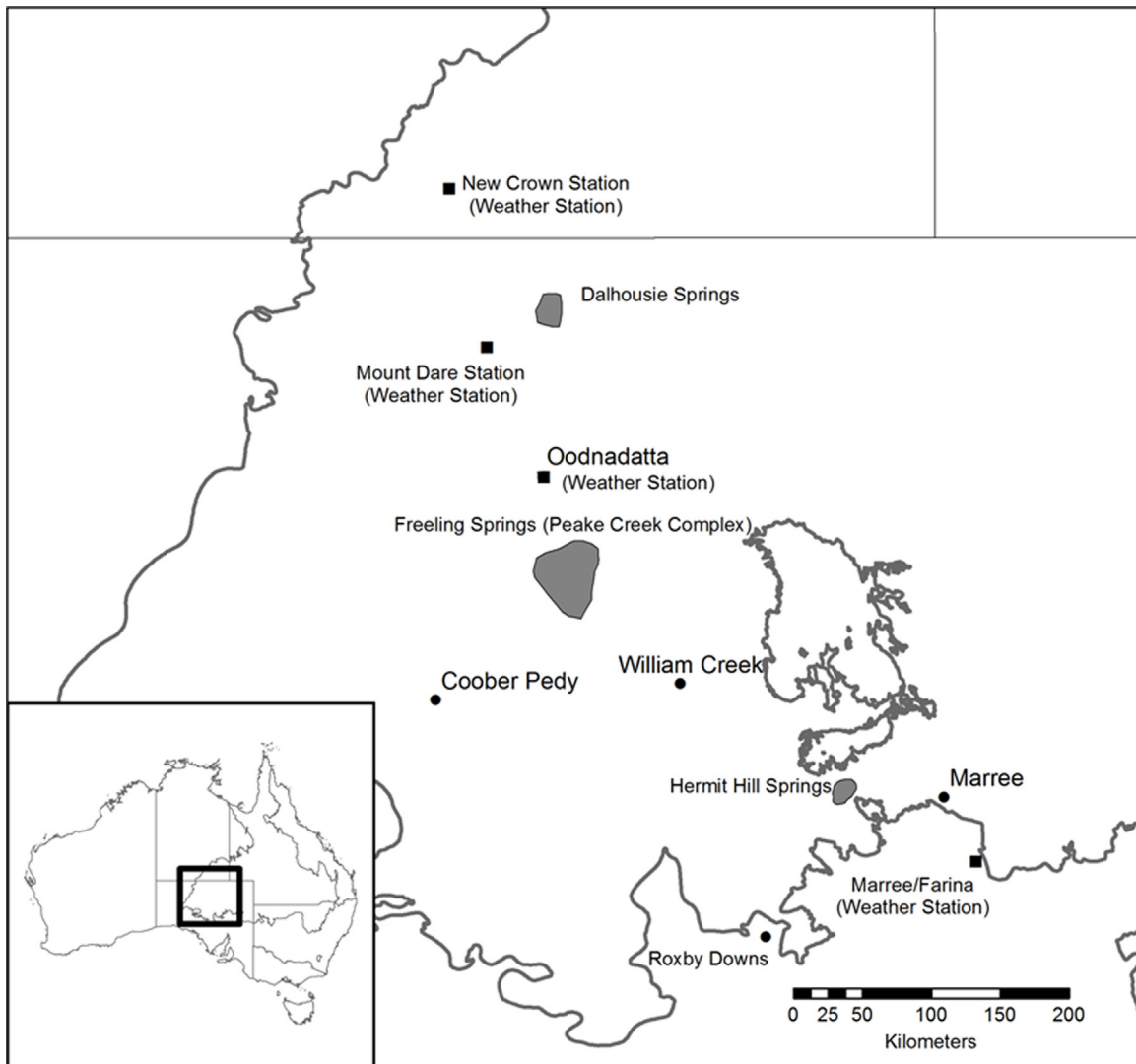
Fig. 2. Study area including the Great Artesian Basin and location of Dalhousie Spring Complex, Freeling South Spring Group, and Hermit Hill Spring Group. Spring groups are clusters of springs that share similar water chemistry and source their water from the same fault or structure; and spring complexes comprise clusters of spring groups that share similar geomorphological settings and broad similarities in water chemistry (Gotch, 2013).

distribution. The long history and isolation of the springs has led to the natural preservation of many endemic, rare and relict flora and fauna (Fensham et al., 2010; Gotch et al., 2008; Guzik et al., 2012; Murphy et al., 2010) of great ecological, evolutionary and biogeographical importance (Lewis et al., 2013).

This study investigated three sites representative of the range of spatial extent and distribution of GAB spring wetlands, and of contrasting vegetation composition, surface formation, geomorphological and hydrogeological settings: Dalhousie Spring Complex (DSC), Freeling Spring Group (FSG), and Hermit Hill Spring Group (HHSG) (Figs. 1 and 2). The most notable difference between these sites is the spatial extent of the artesian springs; those at DSC are more than an order of magnitude larger than at FSG or HHSG, the latter having the least extensive and lowest flowing springs. In addition, the sites contrast in ecological composition, cultural significance, hydrogeological formation and vulnerability to groundwater extractions and land use impacts.

DSC was selected for this study because of its ecological and conservation importance within Australia and internationally. It lies within Witjira National Park and was registered in the Australian National Heritage List implemented under the Environment

Protection and Biodiversity Conservation Act 1999. The complex covers approximately 19,000 ha, situated at latitude 26.45°S and longitude 135.51°E, on the South Australian-Northern Territory border and 50 km west of the western edge of the Simpson Desert in South Australia (SA) (Fig. 2). The regional climate is arid, with low annual rainfall and high temperatures (Table 1).

The 145 springs at DSC are supported by the natural outflow of the GAB at an estimated $0.625\,m^3/s$ (Gotch et al., 2006; Williams and Holmes, 1978). The springs are low features attaining heights of 6 m and widths of 180 m (Clarke et al., 2007). The spring tails are mostly linear in form, extending up to 5 and even 10 km from source, supporting extensive wetlands (White et al., 2013). Love et al. (2013) report that the most plausible mechanism for Permian and Cretaceous aquifer discharge at Dalhousie is through north–northeast trending fault-associated fractures in the McDills–Dalhousie Ridge anticline. Fracturing associated with inter-formational faulting permits both mixing of groundwater as well as discharge of groundwater at surface to form the spring complex. Intermittent river recharge from the Finke River system 150 km northwest of the complex to the Canda-owie Formation (J aquifer) also plays a notable role in sustaining the DSC spring discharge (Love et al., 2013).

Table 1
Summary of mean annual rainfall and mean monthly minimum and maximum relative humidity and temperature for weather stations closest to the study sites. Data sourced from the Australian Bureau of Meteorology.

Study site	Weather station	Mean annual rainfall (mm)	Mean monthly relative humidity (%)	Mean monthly temperature (°C)
Dalhousie Spring Complex & Freeling Spring Group	Oodnadatta Airport	176.8	18–37	5.8–37.9
Hermit Hill Spring Group	Marree/Farina	162.8	24–49	4.1–35.5

DSC (Figs. 1 and 2) has the largest flowing discharge of spring complexes in the Australian arid zone portion of the GAB, and is second only to spring complexes and groups in the far north of Cape York (Gotch, 2013). The discharge rates at DSC are strongly influenced by the potentiometric surface which ranges from over 50 m to less than 5 m in different parts of the complex. This variation is not due to surface topography alone; flows are greatest in the northern half of DSC where there is a wider range in spring elevations, but are also influenced by large aquifer pressure variations, most likely due to the complex geology below DSC (Gotch, 2013; Pers. Comm. T. Gotch; Green et al., 2013).

The wetland communities comprise dense stands of White Tea Tree (*Melaleuca glomerata*) closest to spring outflows and vents, giving way to extensive stands of Common Reeds (*Phragmites australis*) in the upstream permanent swamps, and sparser communities of rushes and sedges on the furthest reaches of the flows. These terminal wetlands are often ephemeral in nature as spring flow fluctuates over time (Lewis et al., 2013; White and Lewis, 2011).

FSG is situated within the Mt. Denison Spring Complex lying immediately to the east of the Denison Ranges at latitude 28.06°S and longitude 135.91°E (Figs. 1 and 2; Table 1). FSG formed along the Kingston fault and abuts the eastern side of the Peake and Denison Inlier, a small range of outcropping Neoproterozoic basement rock (Rogers and Freeman, 1994; Wohling et al., 2013). FSG consists of 100 outflow vents in an almost north-south alignment, the groundwater discharge being fed by mountain system recharge and groundwater from the J Aquifer (Wohling et al., 2013). The spring formations comprise abutment seeps along the edge of the ranges and carbonate mounds, pools and terraces. Most of the springs are small to moderate in size, although several vents have extensive tails extending up to 1.5 km from their source (White et al., 2013). Several species of wetland vegetation are dominant including Common Reed in dense monospecific stands surrounding some spring vents and sparser stands of Common Reed mixed with sedges dispersed along spring outflow tails where standing and free flowing water is present (White et al., 2013).

HHSG is situated within the Hermit Hill Spring Complex (HHSC) centred around the northern portion of Hermit Hill, an outcrop of the Adelaide Geosyncline, located at latitude 29.06°S and longitude 137.41°E (Figs. 1 and 2; Table 1). Hermit Hill Creek encircles the east and northerly flanks of Hermit Hill, its course bisecting HHSG. HHSG consists of 429 vents forming an elongated arc between the base of Hermit Hill and the intermittent creek. Spring wetlands, tens of metres in extent, comprise dense stands of Common Reed with several species of lower lying sedges traversing the interconnected spring tails. Smaller clusters of interconnected springs occur at the base of the outcrop and are likely to be fed from its runoff, similar to the mountain system recharge at Mt. Denison (White et al., 2013). HHSG is within the impact zone of Wellfield A, from which mining company BHP Billiton has extracted an average of 1892 ML/annum of artesian water for the Olympic Dam mine since Wellfield B came online in 1997 (BHP Billiton, 2014).

2.2. Image data and pre-processing

QuickBird and WorldView-2 Very High Resolution (VHR) multi-spectral satellite images were acquired for the three sites to develop the image Normalised Difference Vegetation Index (NDVI) calibration and wetland area discharge rate relationships (Table 2 and Fig. 3). The images were provided partially orthorectified (coarse terrain corrections and projected to a constant base elevation) and partially radiometrically corrected (DigitalGlobe, 2013). Positional errors were less than 10 m for the QuickBird imagery and 6.5 m for the WorldView-2 imagery; further geo-registration was performed to improve positional accuracy for aligning the imagery with field survey plots. Further radiometric correction was conducted to convert the images to apparent surface reflectance using a modified MODerate spectral resolution atmospheric TRANSmittance (MODTRAN) algorithm, Fast Line-of-sight Atmospheric Analysis of Spectral Hypercubes (FLAASH) in the Atmospheric Correction Module of ENVI V.5.0 (EXELIS Visual Information Solutions, Boulder, CO) remote sensing software (DigitalGlobe, 2013; Cook et al., 2009). The satellite scene tiles were subsequently colour balanced and mosaicked to give full seamless coverage for each site. ENVI V5.0 software was used for this and subsequent image analysis.

Digital colour (red, green and blue) aerial photography at 0.3 m GSD was acquired in March 2009 for all three sites. The high resolution photography was used to assist with interpretation of the wetland extent mapping from the VHR satellite image analysis.

2.3. Vegetation survey and spring discharge measurements

Vegetation surveys were conducted in sample plots representative of the range of vegetation types and cover for each spring group or complex. The timing of these surveys (DSC in March 2009, FSG in May 2011, and HHSG in April/May 2011) corresponded with the satellite image acquisitions as closely as possible (Table 2 and Fig. 4). For FSG the field survey and image acquisition were concurrent, at DSC the imagery was acquired 3–4 weeks after field survey, while at HHSG there was an eight week lag between field survey and image acquisition, unavoidable because of prolonged cloudy conditions preventing cloud-free image acquisition. Rainfall at the meteorological stations nearest the study sites is also shown in Fig. 4 (New Crown and Hamilton station proximal to DSC; Oodnadatta Airport proximal to FSG; Marree (Farina) proximal to HHSG). The DSC imagery and field survey occurred after a prolonged period of low rainfall, while those for FSG occurred after two major rainfalls (10 and six weeks prior). At HHSG the field survey was conducted April/May 2011 after major rainfalls in February and April 2011, with little further rain prior to the later satellite image acquisition.

Vegetation cover and composition were recorded within plots of 9 × 9 m, designed to allow for geolocation errors and geometric accuracy of the imagery, as well as the scale of vegetation stands and variation. A total of 11 sample plots were recorded at DSC, 18 at FSG, and 32 at HHSG (Fig. 3). Within the plots, percentage cover of plant species and overall fractions of photosynthetic vegetation, dry vegetation, water and soil were recorded using the methods

Table 2
Summary of technical specifications of satellite imagery used in this study. GSD refers to Ground Sample Distance.

Sensor	Site	Date captured	GSD	Waveband configuration
QuickBird	DSC	6th May 2009	2.62 m	479.5 nm—blue; 546.5 nm—green; 654.0 nm—red; 814.5 nm—near-infrared
WorldView-2	FSG	9th May 2011	1.85 m	427 nm—coastal; 478 nm—blue; 546 nm—green; 608 nm—yellow; 659 nm—red;
	HHSG	25th June 2011		724 nm—red-edge; 831 nm—near-infrared 1; 908 nm—near-infrared 2

described by White et al. (2013) and White and Lewis (2011). Differential GPS locations were recorded at the corners of the survey plots to enable their later identification on the imagery.

Spring flow data were selected either from ongoing monitoring records or new *in-situ* measurements that were made for this study. The *in-situ* flow measurements coincided with the vegetation surveys. The timing of the discharge measurements corresponded as closely as feasible with the satellite image acquisitions.

At DSC weir flow gauge data were obtained from the South Australian Department of Environment, Water and Natural Resources (DEWNR) for four weirs (Fig. 3). This data consisted of current meter discharge records taken on a biannual basis. In addition, salt dilution measurements of flow for three additional springs (Fig. 3) were obtained in July 2009 (White and Lewis, 2013; Wolaver et al., 2013). At HHSG spring discharge data for April 2011 were selected from biannual monitoring weir flow gauge records taken by BHP Billiton (2013b) at this site (Fig. 3).

In addition, *in-situ* spring surface flows were measured in April/May 2011 for FSG and HHSG using a combination of two methods (Fig. 5). For free-flowing springs with surface outflow of more than approximately 10 l/m a salt dilution method was applied, which is an adaptation of the slug-injection method (Green and Berens, 2013; Kilpatrick and Cobb, 1985). For flowing springs of lower outflow rates (less than 10 l/m), an alternative method was necessary. In these cases, the spring surface flow was carefully channelled to a collection point using a combination of plastic screens and sandbags. At the collection point a small hole was dug to fit a container which collected all channelled flow, ensuring that minimal flow escaped (Fig. 6). The rate of fill of the container was recorded three or more times and a mean rate of flow calculated, which equated to the approximate rate of surface flow through the channel (Green and Berens, 2013).

Flow measurements, using either of the methods described above, were taken in channels at points where flowing water emerged from the vegetated spring mound (Fig. 5). Total spring discharge rates were calculated from the sum of surface flow occurring at the point(s) of measurement (Green and Berens, 2013). It is acknowledged that some subsurface flow away from the spring discharge point may occur in many of these springs and this is not included in the estimate of flow by these methods. However, it is assumed that, due to the very low velocity of subsurface flow, this forms only a minor component of the flow from the discharge point (Green and Berens, 2013).

For DSC eight flow records were selected for comparison of spring flow rate and wetland area (White and Lewis, 2011). A total of 20 and 24 spring flows were recorded for FSG and HHSG, respectively.

2.4. Delineating wetland extent

The QuickBird and WorldView-2 satellite images were analysed to precisely delineate the extent of spring-fed wetlands and develop calibration relationships with on-ground vegetation cover using the methods described by White and Lewis (2011). NDVI was applied using the red (654.0 nm) and near infrared (814.5 nm) bands of the QuickBird imagery, and the red (659 nm) and infrared I (831 nm) bands of the WorldView-2 imagery. The wavebands selected for the WorldView-2 image NDVI analyses corresponded most closely with those of the QuickBird sensor.

For each site, regression analysis was used to determine the relationship between satellite image NDVI and percentage vegetation cover measured in corresponding 9 × 9 m field sample plots. For DSC overall vegetation cover (photosynthetic and dry vegetation) was used to develop the regression relationship (White and Lewis, 2011). This approach was refined for FSG and HHSG where the photosynthetic vegetation fraction of cover was used for the analyses. From these relationships NDVI thresholds were determined for each site to separate wetland vegetation from surrounding dryland vegetation.
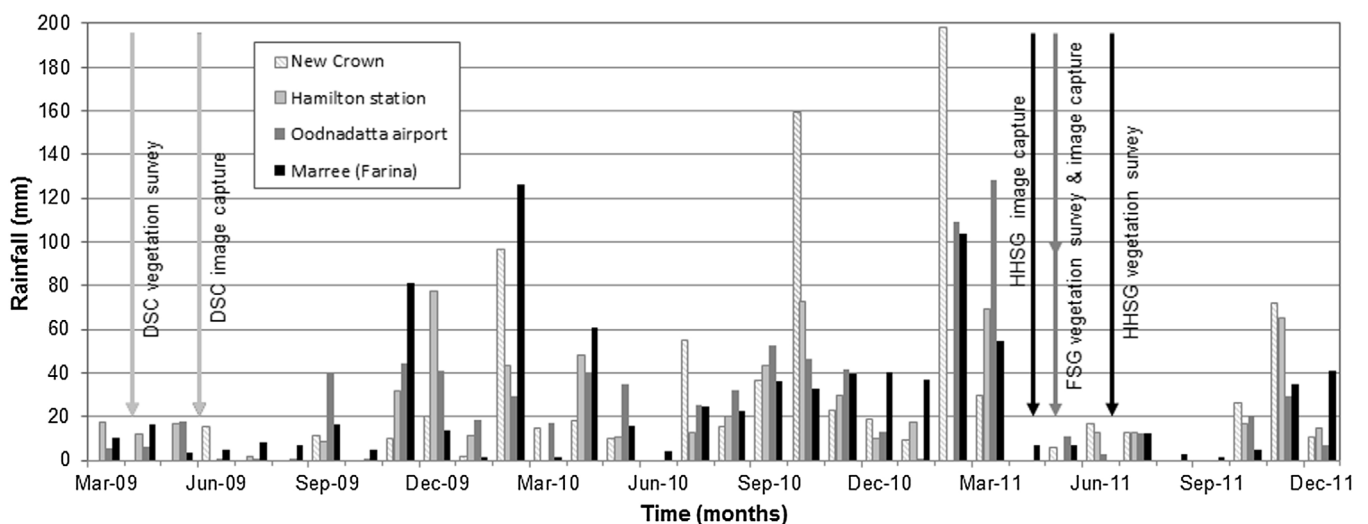

Fig. 3. Australian Bureau of Meteorology automatic weather station monthly rainfall data for New Crown, Hamilton station, Oodnadatta Airport, and Marree/Farina; locations on Fig. 2. Black arrows indicate image capture dates and grey arrows vegetation survey dates for each site.
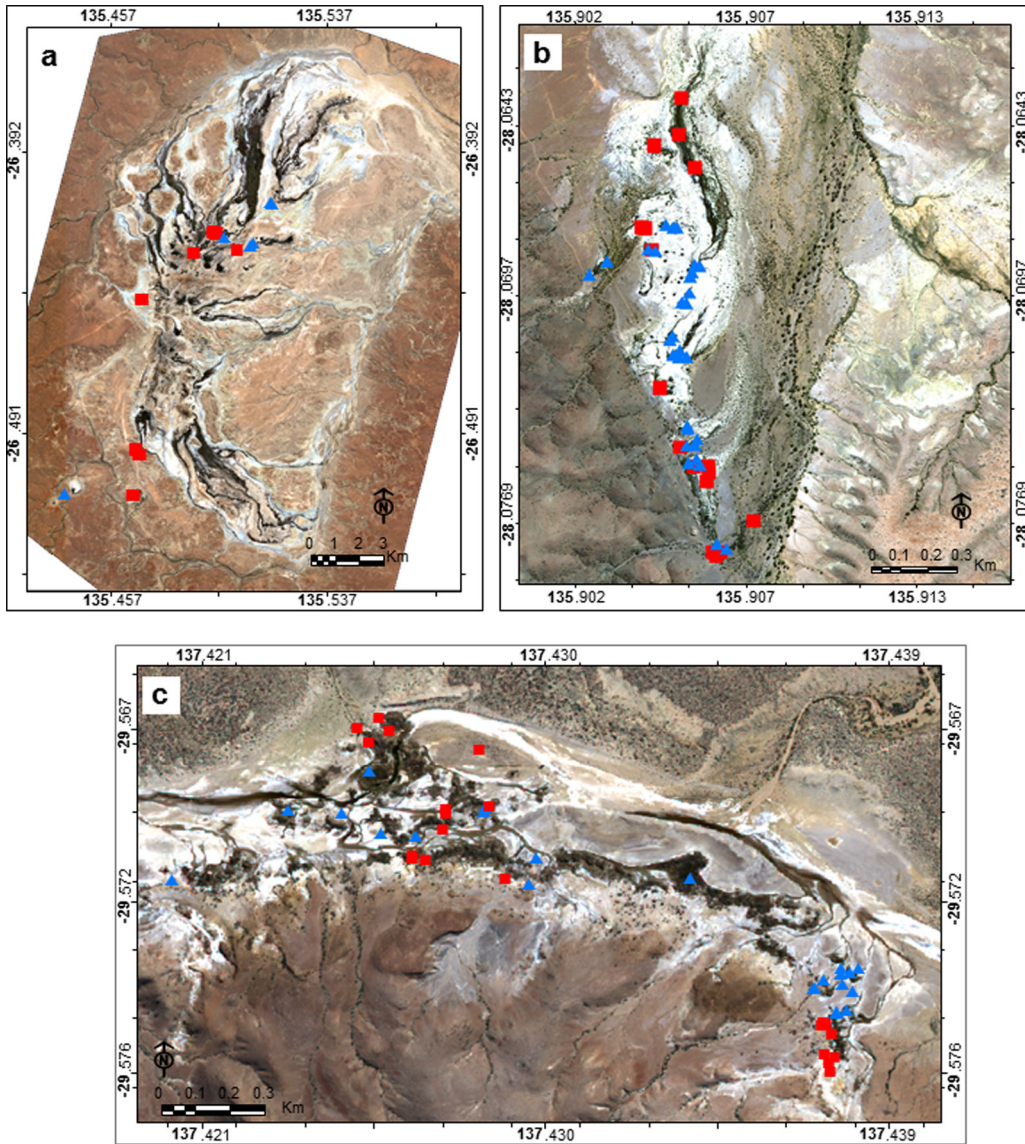
Fig. 4. Study areas: (a) Dalhousie Spring Complex; (b) Freeling Spring Group; (c) Hermit Hill Spring Group; including location of vegetation sample plots (red squares—not to scale) and spring discharge measurements (blue triangles—not to scale).

2.5. Wetland extent-spring flow relationships

The methodology developed by White and Lewis (2011) for DSC was applied to FSG and HHSG using the WorldView-2 satellite imagery. This involved the following: (i) wetland area for each spring was delineated by heads-up digitising on the NDVI threshold imagery; (ii) where springs were interconnected, their associated wetlands were distinguished using a suite of ancillary
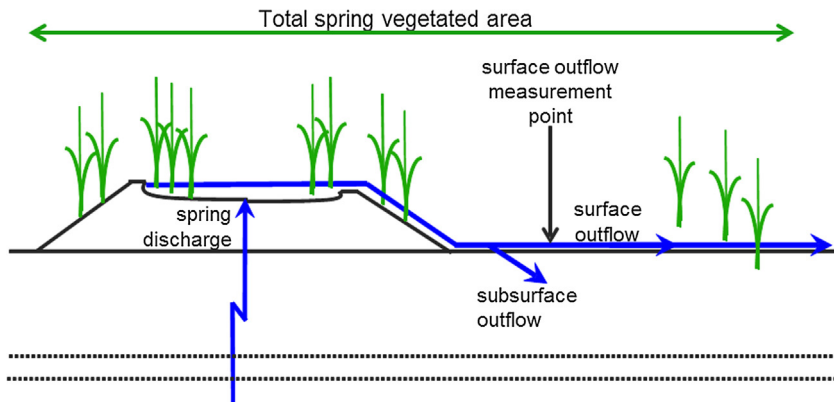

Fig. 5. Conceptual model of spring wetland area relative to the outflow measurement, along with water flux pathways, in a typical mound spring.

Fig. 6. In-channel measurement of spring surface flow, used where flow rates were less than 0.167 l/s (10 1/min). The rate of filling of plastic container was measured three or more times and a mean flow rate calculated.

data, including spring vent DGPS coordinates (Gotch, 2010; Lewis et al., 2013), proximity to spring flow monitoring locations, and expert knowledge of the sites; (iii) polygons produced from the digitising were intersected with the NDVI threshold image to produce precise delineations of wetland extent for the springs of interest; and (iv) individual spring wetland areas were calculated.

A non-parametric Kruskal–Wallis test was used on ranked wetland extent data for the selected sample wetlands at all three sites. This test determined if the wetland areas for the three sites were taken from populations with the same distributions, *i.e.*, they share the same continuous distribution. To determine the relationship between groundwater flow rate from springs and the area of wetland vegetation supported by them regression analyses were performed for the three sites. Analysis of Covariance (ANCOVAR) was used to assess whether there are statistical differences between the resultant regression relationships for DSC, HHSG, FSG.

3. Results

3.1. Image NDVI-ground vegetation cover relationships

The range of NDVI derived from the VHR satellite imagery differs somewhat between the three sites, ranging between 0.11–0.73 (DSC), 0.23–0.8 (FSG), and 0.11–0.56 (HHSG). Their associated on-ground vegetation covers also differ. A restricted range of on-ground photosynthetic vegetation cover is notable for HHSG (5–45%), while the other sites exhibit broader ranges of vegetation cover; between 4–87% (DSC—dry and photosynthetic cover) and 15–80% (FSG—photosynthetic cover) (Fig. 7).

An increase of NDVI with increasing vegetation cover is evident at all sites, despite these differences in ranges of NDVI and on-ground vegetation cover. The increase in NDVI with vegetation cover also corresponds with differences in vegetation community composition: perennial vegetation, in particular Common Reed, has high NDVI (DSC 0.56–0.73; FSG 0.80; HHSG 0.09–0.39—for mixed perennial and ephemeral vegetation); ephemeral spring tail vegetation exhibits a wider range of moderate NDVI (DSC 0.37–0.51; FSG 0.37–0.65; HHSG 0.15–0.56); and surrounding dryland vegetation generally shows much lower NDVI (DSC 0.11–0.32; FSG 0.23–0.65; HHSG 0.14–0.15).

Ephemeral and mixed spring tail vegetation at FSG and HHSG are most variable in both NDVI and vegetation cover. For FSG spring tail vegetation exhibits a wide range of NDVI and associated vegetation cover. HHSG reflects a similar trend. A notable difference which is apparent for spring tail vegetation between FSG and HHSG is the relatively lower NDVI at HHSG compared to FSG for vegetation cover.

Strong to good regression relationships between image NDVI and corresponding on-ground percentage cover are evident for DSC and FSG ($R^2 = 0.86$, $R^2 = 0.59$, $p < 0.001$) (Fig. 7). A weaker, but still significant regression relationship is evident for HHSG ($R^2 = 0.49$, $p < 0.001$). There is little difference between the three sites in the slope of the regressions (DSC 0.007; FSG 0.006; HHSG 0.007) (Fig. 7).

On the basis of the NDVI-vegetation cover relationships thresholds were established for each site above which NDVI values were considered to be indicative of wetland vegetation with >30% fractional cover of photosynthetic vegetation (Fig. 7). This value enabled detection of the wetland vegetation at a per pixel scale, given that the vegetation plots were 9×9 m. The thresholds are very similar for all sites: DSC 0.35; FSG 0.33; HHSG 0.32.

3.2. Inter-site variation of wetland extent

The spatial extent and distribution of the wetlands at the three sites was characterized and quantified from the NDVI thresholds applied to the VHR satellite imagery. The total mapped wetland area varies by over an order of magnitude between DSC at 913 ha, to 9.4 ha at FSG, and 9 ha at HHSG (Fig. 8). All sites have a wide range of spring spatial extents and one very large spring which dominates the overall wetland area. The largest springs at each site range from 189.2 ha at DSC extending almost 10 km; 2.93 ha for FSG with an extent of several kilometres; and 1.37 ha at HHSG for 'The Fen' extending up to tens of metres.

In addition to these overall differences in wetland extent between the three spring groups, there were corresponding differences in wetland areas for the springs used for the flow/wetland area regressions. The Kruskal–Wallis test revealed significant differences between the three spring groups in the areas of the sample wetlands ($H = 19.339$, $p = 0.05$). The three sets of wetland areas had mean ranks of 50.0 (DSC), 24.48 (FSG), and 22.84 (HHSG), indicating that the DSC spring areas used in the analysis were much larger than those for the other spring groups.

3.3. Wetland extent spring discharge relationships

The spring discharges also differed between sites. The range of discharge rates measured at FSG is small; the majority flows were less than 0.5 l/s and the maximum flow recorded at 2.09 l/s. Discharge rates measured at HHSG are of a similar order of magnitude to those at FSG, ranging from a minimum of 0.001 l/s to a maximum of 1.16 l/s. By contrast, the DSC discharge rates are two orders of magnitude greater, ranging from 0.7 to 1427 l/s.

Despite these differences strong positive linear relationships were developed between spring wetland area and discharge at the individual spring level for all three sites (DSC $R^2 = 0.99$; FSG $R^2 = 0.95$; HHSG $R^2 = 0.92$; $p < 0.001$ in all cases; Fig. 9). There are some differences in the relationships between the sites. For DSC wetland area (ha) is approximately 1.21 times the discharge rate (in m^3/s), at HHSG wetland area is 0.68 of spring flow, and at FSG spring wetland area is approximately 2.58 times the spring discharge
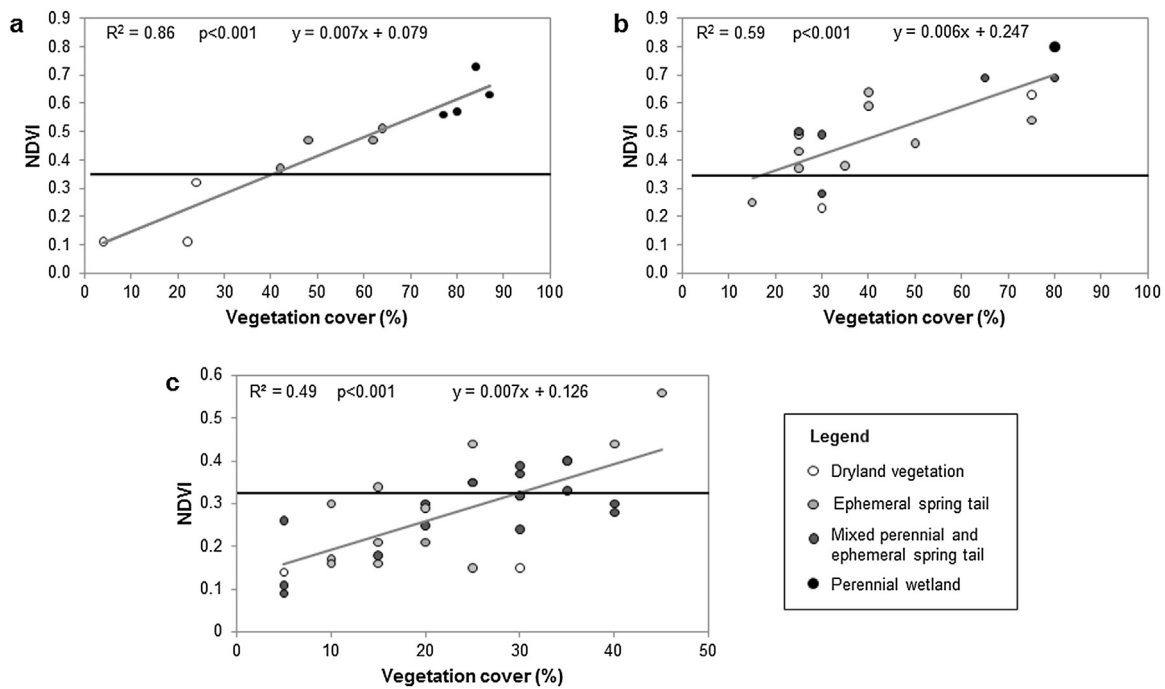
Fig. 7. Regressions of NDVI against vegetation cover at the three sites: (a) Dalhousie (11 sample plots); (b) Freeling (18 sample plots); and (c) Hermit Hill (32 sample plots). The thick black lines represent NDVI thresholds of 0.35, 0.33, and 0.32, respectively.

rate. However analysis of covariance (ANCOVAR) indicated that the slopes of the three regression lines for the three sites are not significantly different ($F_{2,46} = 0.434$, $p = 0.651$). A very strong positive linear regression relationship was also apparent between spring wetland area and discharge for all sites combined ($R^2 = 0.99$ $p < 0.001$).

However, there is some deviation from the regression lines for some of the springs. Most notable are outlying values at DSC, particularly for springs with lower discharge rates, which were lower relative to their computed wetland areas (Fig. 9). These springs ranged from the lowest discharge of 0.071 l/s with an associated wetland area of 2.7 ha to a discharge rate of 0.57 l/s with an associated wetland area of 9.4 ha. HHSG also exhibits a few springs which deviate from the regression, with discharge rates relatively higher than their respective wetland areas. The most notable outliers at HHSG are springs with discharges of 0.057 and 0.199 l/s with associated lower wetland areas of 0.017 and 0.034 ha, respectively.

4. Discussion

4.1. Image NDVI-ground vegetation cover relationships

The overall trend of increasing image NDVI with corresponding increases in on-ground vegetation cover for all sites indicates the robustness of NDVI for the range of vegetation communities present within these GAB springs. The similar inter-site trend is consistent with the response of NDVI for spring vegetation computed from Moderate Resolution Imaging Spectroradiometer (MODIS) time series data reported by Petus et al. (2013).

Perennial wetland vegetation exhibits relatively high NDVI across all sites. Lower NDVI for perennial vegetation at HHSG can be explained by a satellite image capture late in the growing season (25th June 2011) and the lag between image capture and on-ground vegetation sampling with senescence of the plants (eight weeks). Over this period Common Reed progressively senesces from its summer maximum greenness and growth, as documented by Petus et al. (2013). This outcome was accentuated by two major rainfall events prior to the vegetation sampling in April/May 2011, followed

by a notable dry period prior to satellite image capture (Fig. 3). Lower NDVI may also be indicative of the differing community composition at HHSG, with a variety of dominant ephemeral sedges and marginal saline species present with sparser cover (Fig. 1c). This would explain the 10–37% difference in the coefficient of determination (R^2) of the regression relationship between HHSG and the other sites.

The ephemeral and mixed ephemeral and perennial spring tail vegetation exhibits the most wide-ranging NDVI and corresponding vegetation covers for FSG and HHSG. The main driver for this variation is the variability of spring tail flow paths causing preferential wetting and drying of the adjacent vegetation, being highly dynamic over short time periods, 2–3 years, (White and Lewis, 2011), in response to rainfall and land management. The use of only the photosynthetic vegetation fraction of cover at FSG and HHSG may also contribute to these differences, particularly the reduced range of NDVI at HHSG.

The NDVI thresholds established to delineate spring wetland vegetation from the surrounding dryland vegetation are very similar for all sites. These thresholds represent springs under wet and dry conditions, as well as incorporating their wide diversity. The thresholds generally delineated wetland vegetation with >30% photosynthetic cover fractions (Fig. 7). Therefore, in future it may not be necessary to establish a calibration relationship between image NDVI and on-ground vegetation cover for continued monitoring. A similar threshold can be applied to NDVI calculated from VHR satellite imagery captured over other arid springs, reducing the need for on-ground vegetation sampling. This improvement in monitoring capabilities is pertinent for these remote, isolated, and geographically disparate wetland ecosystems.

4.2. Inter-site variability of wetland extent

The spatial extent and distribution of the spring wetlands derived from the satellite image NDVI threshold vary considerably between sites. The most striking difference is the extent of the wetlands, with an order of magnitude difference. The relative
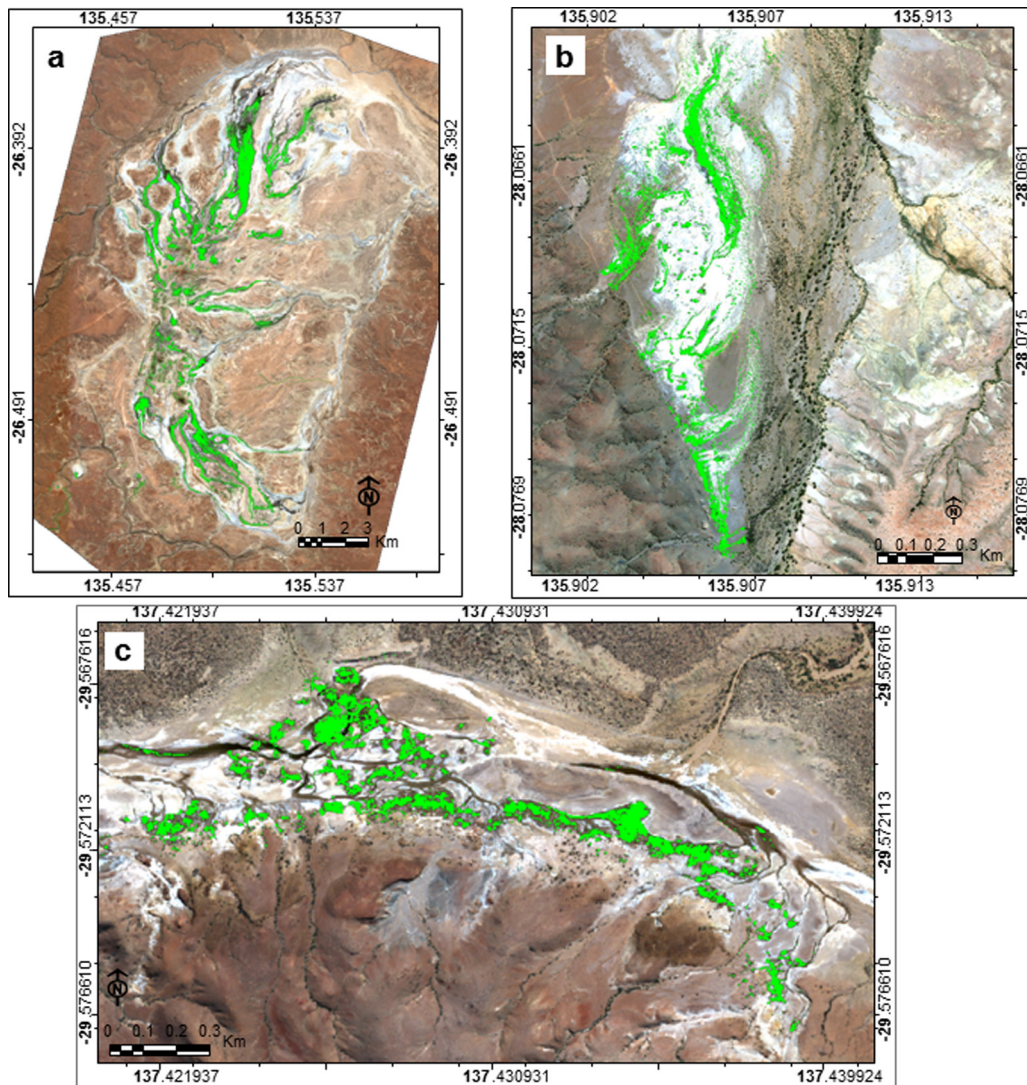
Fig. 8. Extent and distribution of wetland area, based on 0.35, 0.33, and 0.32 NDVI thresholds (green regions), for QuickBird and WorldView-2 satellite imagery acquired over the three sites: (a) Dalhousie 6th May 2009; (b) Freeling 9th May 2011; and (c) Hermit Hill 25th June 2011.

sizes of the selected sample wetlands followed a similar trend, with those at DSC statistically much larger than the other two sites, confirmed by a Kruskal–Wallis test. This provides strong evidence that the NDVI-threshold approach can be applied successfully to spring wetland extents differing by orders of magnitude. These differences are primarily due to the differing hydrogeological settings of the sites, resulting in a wide range of discharge rates supporting the spring wetlands. These differences in wetland extents between sites concur with those reported by Holmes et al. (1981), which they attribute to changes in overall discharge and evaporation rates varying throughout the year and grazing impacts. Other influences on the extent and spatial distribution of the spring wetlands at the sites include changes in land use at DSC (date palm removal and lightning strike leading to burning and regrowth of spring vegetation, White and Lewis, 2011); grazing impacts at DSC and FSG (reducing wetland extents); and at HHSG potential impacts from water extraction for mining operations at the Olympic Dam mine.

4.3. Wetland extent spring flow relationship: Inter-site variability

White and Lewis (2011) established a strong direct relationship between individual spring wetland extent and groundwater discharge rates using satellite imagery. This confirmed the potential of the technique for monitoring spring flows and concurred with Williams and Holmes (1978) findings. The results of the current study replicate this strong linear relationship at two additional sites, FSG and HHSG. These sites contrast in discharge rates, hydrogeological recharge and discharge mechanisms, geomorphological characteristics, landscape settings and vegetation community composition.

The highest flows and most extensive wetlands at DSC were recorded in May–June 2010, following a period of high rainfall (Fig. 3) and under these conditions the wetland area/flow relationship is closer to that calculated for FSG (White and Lewis, 2013). Satellite image capture was near-coincident with the ground vegetation surveys at FSG (9th May 2011) following the high rainfalls in the region, which would contribute to the greater slope of 2.68, indicating spring wetland areas are generally larger than flow rates (Fig. 9). This is not the case for HHSG, where wetland areas are generally smaller than expected for the spring flow rates, due to the drying off of wetland vegetation during the lag between *in-situ* measurements of vegetation cover and the satellite image acquisition. The drier vegetation provided lower image NDVI values, underestimating spring wetland extents relative to the greener photosynthetic vegetation covers recorded in the field survey. These findings indicate that there is a range of natural
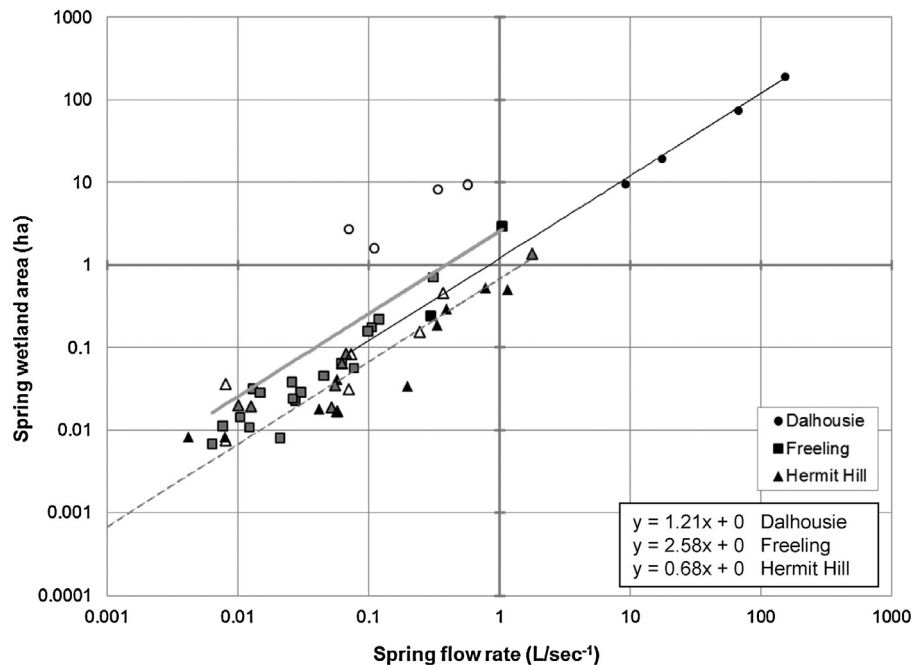
Fig. 9. Regression of wetland areas against spring flow rate for the three sites: (a) Dalhousie May 2009; (b) Freeling May 2011; and (c) Hermit Hill April 2011. Log^{10} scale used to represent order of magnitude differences of spring sizes between sites. Hollow symbols represent salt dilution data, channelled collection point and bucket data, and black solid symbols represent weir gauge data.

variation in the wetland area/flow relationship that encompasses spring variability in response to changing climatic conditions, land use, and aquifer pressure.

The outliers from the regression relationships for DSC and HHSG (Fig. 9), could be attributed to several factors. There is a range of error associated with the different manual flow measurement techniques employed (Carter and Davidian, 1989), which is accentuated for springs with smaller discharge rates. Three of the DSC outlying springs were recorded using different methods, collected in July 2009, two months after the satellite imagery and vegetation surveys. Variability of discharge measurements is compounded by the dynamic nature of the flow channels (Pers. Comm. V. Berens; Williams and Holmes, 1978; White and Lewis, 2011). Holmes et al. (1981) reported similar differences using manual techniques for deriving their relationship. At HHSG greater confidence can be given to discharge measurements recorded at discrete springs clustered around the base of the outcropping Hermit Hill, where BHP Billiton have erected weirs, than the *in-situ* measurements recorded at springs that were inter-connected and often extend over large areas (Fig. 3).

The strong positive relationships between spring flow rate and wetland area replicated at three contrasting sites indicates the suitability of this technique for a wide range of springs. ANCOVAR revealed no statistically significant differences in the slopes of the regressions between the three sites. This finding provides stronger evidence that this relationship can be established for a wide range of spring flows and associated wetland areas. The larger number of observations at FSG (21) and HHSG (25) increases our confidence in this approach. Consequently, wetland area can be used as a surrogate for spring flow volume, providing an objective and cost-effective means for monitoring spring response to changes in aquifer pressure, land use and climate. Although the precise regression relationship, in particular the gradient of the slope, varies with spring setting and preceding rainfalls, these differences are not statistically significant (White and Lewis, 2011). Continued monitoring using this approach will allow the range of variation in this relationship to be estimated. Temporal context

can be achieved using a multi-sensor approach, placing short-term variations within longer-term trends. For example, Petus et al. (2013) demonstrate the natural range of inter and intra-annual variation of spring wetlands using long time series MODIS NDVI satellite imagery.

5. Conclusions

The current paper addresses the need for a more generalizable methodology for assessing and monitoring arid GAB spring flows, with less reliance on site-specific ground-based calibration, providing a remote monitoring tool which is repeatable and consistent over space and time. Such tools are necessary and timely given the significance of the Australian GAB as a water resource and the ecological importance of its wetlands, particularly in light of increasing water demands for mining.

Regression relationships between image NDVI and on-ground vegetation cover for the sites revealed consistent increasing NDVI with increasing vegetation cover. Thresholds based on this relationship, which delineated the spring wetland vegetation from surrounding dryland vegetation, fell within a very narrow range for the three sites investigated. The regression relationships and derived thresholds represent the GAB springs under wet and dry antecedent conditions and incorporate the wide diversity in their scale, geomorphology, hydrogeology and vegetation community composition. Consequently, it may not be necessary to establish site-specific calibration relationships between image NDVI and on-ground vegetation cover for continued monitoring of spring wetlands. This significant finding reduces the need for on-ground validation of image-based wetland mapping for future springs monitoring.

Detailed delineation and quantification of groundwater-fed wetlands from satellite imagery was directly related to *in-situ* measurements of discharge rates for all of the sites investigated. The slopes of these regression relationships were not significantly different. The replication of these strong positive relationships at contrasting sites demonstrates that this technique can be

applied to a wide range of springs with differing spatial scales and landscape settings. Wetland area measurements of springs can provide a surrogate for *in-situ* flow records that are often difficult to consistently obtain and maintain over time in these remote areas. Continued monitoring will allow an estimate of the range of variation in the wetland area/flow relationship that encompasses natural spring variability. This approach can then be supported by monitoring longer-term trends, defining the natural variation in entire spring wetlands over time, derived from hyper-temporal moderate resolution satellite imagery (Petus et al., 2013). A multi-sensor approach is essential to improve our understanding of the response of spring wetlands to anthropogenic influences and climate change interactions.

This study also provides new, objective baseline documentation of the status and distribution of the springs at DSC, FSG and HHSG. This information can be compared with future monitoring using the approaches proposed in this paper and the change detection techniques demonstrated in White and Lewis (2011). Such an approach will also provide new insights into the interplay of a range of impacts on the springs and their groundwater discharge, including climate change, natural hazards, land use changes, grazing, groundwater extractions and aquifer pressure changes.

Acknowledgements

Appendix A. Supplementary data

Supplementary data associated with this article can be found, in the online version, at http://dx.doi.org/10.1016/j.ecolind.2015.01.032.

References

Ah Chee, D., 2002. Kwatye, indigenous peoples connection with kwatye (water) in the Great Artesian Basin. Environ. S.A. 9, 20–21.

BHP Billiton, 2013a. Monitoring Program—Flora. BHP Billiton, Viewed 7 April 2014, ⟨http://www.bhpbilliton.com/home/aboutus/regulatory/Documents/_copper/olympicdam/130717_Copper_OlympicDam_2664MonitoringProgramFlora2013.pdf⟩.

BHP Billiton, 2013b. Monitoring Program—Great Artesian Basin (GAB). BHP Billiton, Viewed 7 April 2014, ⟨http://www.bhpbilliton.com/home/aboutus/regulatory/Documents/_copper/olympicdam/130717_Copper_OlympicDam_2789MonitoringProgramGreatArtesianBasinGAB2013.pdf⟩.

BHP Billiton, 2014. Annual Environmental Protection and Management Program Report: 1st July 2013 to 30th June 2014, Report to The Governement of South Australia. BHP Billiton, Olympic Dam, Australia.

Carter, R.W., Davidian, J., 1989. Techniques of Water-Resources Investigations of theUnited States Geological Survey. Applications of Hydraulics, Book 3. United States Government Printing Office, USA, pp. 1–13.

Clarke, J., Bourke, M., Nelson, P., Manga, M., Fonseca, J., 2007. The Dalhousie Mound Spring Complex as a guide to Martian landforms, processes and exploration. In: Mann, D.G. (Ed.), Proceedings of the 7th Australian Mars Exploration Conference. Mars Society Australia, Clifton Hill, Vic.

Cook, B.D., Bolstad, P.V., Naesset, E., Anderson, R.S., Garrigues, S., Morisette, J.T., Nickeson, J., Davis, K.J., 2009. Using LiDAR and Quickbird data to model plant production and quantify uncertainties associated with wetland detection and land cover generalizations. Remote Sens. Environ. 113, 2366–2379.

Cox, R., Barron, A., 1998. Great Artesian Basin Resource Study. Great Artesian Basin Consultative Council (GABCC), Manuka, Australia.

Department of Sustainability, Environment, Water, Population, Communities, 2011. The Community of Native Species Dependent on Natural Discharge of Groundwater from the Great Artesian Basin. Community and Species Profile andthreats Database, Canberra, Australia.

DigitalGlobe, 2013. DigitalGlobe's Core Imagery Product Guide. DigitalGlobe.

Fensham, R.J., Ponder, W.F., Fairfax, R.J., 2010. Recovery plan for the community of native species dependent on natural discharge of groundwater from the Great Artesian Basin. In: City East (Ed.), Basin. Report to Department of the Environment, Water, Heritage and the Arts, Canberra. Queensland Department of Environment and Resource Management, Brisbane. C. East, pp. 1–58.

Gotch, T.B., 2010. Great Artesian Basin Springs of South Australia: Spatial Distribution and Elevation Map. South Australian Arid Lands Natural Resources Management Board, Adelaide, Australia (Last Updated June 2010).

Gotch, T.B., 2013. Spatial survey of springs. In: Lewis, M.M., White, D.C., Gotch, T.B. (Eds.), Allocating Water and Maintaining Springs in the Great Artesian Basin. vol IV: Spatial Survey and Remote Sensing of Artesian Springs of the Western Great Artesian Basin. National Water Commission, Canberra.

Gotch, T.B., Adams, M., Murphy, N.P., Austin, A.D., 2008. A molecular systematic overview of wolf spiders associated with Great Artesian Basin Springs in South Australia: evolutionary origins and an assessment of metapopulation structure in two species. Invertebr. Syst. 22, 151–165.

Gotch, T.B., Noack, D., Axford, G., 2006. The green cancer: date palms at Dalhousie springs. In: Proceedings of the 6th GAB Springs Researchers Forum, Adelaide, Australia, pp. 35–57.

Green, G., Berens, V., 2013. Relationship between aquifer pressure changes and spring discharge rates. In: Love, A.J., Shand, P., Crossey, L., Harrington, G.A., Rousseau-Gueutin, P. (Eds.), Allocating Water and Maintaining Springs in the Great Artesian Basin. Vol. III: groundwater discharge of the Western Great Artesian Basin. National Water Commission, Canberra.

Green, G., White, M., Gotch, T., Scholz, G., 2013. Allocating Water and Maintaining Springs in the Great Artesian Basin. Vol. VI: Risk Assessment Process for Evaluating Water use Impacts on Great Artesian Basin Springs. National Water Commission, Canberra.

Guzik, M.T., Adams, M.A., Murphy, N.P., Cooper, S.J.B., Austin, Ad.D., 2012. Desert springs: deep phylogeographic structure in an ancient endemic crustacean (*Phreatomerus latipes*). PLoS ONE 7, e37642, http://dx.doi.org/10.1371/journal.pone.0037642.

Habermehl, M.A., 1980. The Great Artesian Basin Australia. Bur. Miner. Res. J. Aust. Geol. Geophys. 5, 9–38.

Holmes, J.W., Williams, A.F., Hall, J.W., Henschke, C.J., 1981. Measurements of discharges from some of the mound springs in the desert of Northern South Australia. J. Hydrol. 49, 329–339, http://dx.doi.org/10.1016/S0022-1694(81)80017-0.

Keppel, M.N., Clarke, J.D.A., Halihan, T., Love, A.J., Werner, A.D., 2011. Mound springs in the arid Lake Eyre South region of South Australia: a new depositional tufa model and its controls. Sediment. Geol. 240, 55–70, http://dx.doi.org/10.1016/j.sedgeo.2011.08.001.

Keppel, M.N., Wohling, D., Fulton, S., Sampson, L., Karlstrom, K.E., Nelson, G., Ransley, T., Love, A.J., 2013a. Summary of hydrologeology and hydrostratigraphy. In: Love, A.J., Shand, P., Crossey, L., Harrington, G.A., Rousseau-Gueutin, P. (Eds.), Allocating Water and Maintaining Springs in the Great Artesian Basin. Vol. I: Hydrogeological Framework of the Western Great Artesian Basin. National Water Commission, Canberra.

Keppel, M.N., Halihan, T., Love, A.J., Post, V., Werner, A., Clarke, J., 2013b. Formation and evolution of mound springs. In: Love, A.J., Shand, P., Crossey, L., Harrington, G.A., Rousseau-Gueutin, P. (Eds.), Allocating Water and Maintaining Springs in the Great Artesian Basin. Vol. III: Groundwater Discharge of the Western Great Artesian Basin. National Water Commission, Canberra.

Kilpatrick, F.A., Cobb, E.D., 1985. Measurement of Discharge Using Tracers, Techniques of Water-Resources Investigations. US Geological Survey, USA.

Lewis, M.M., White, D.C., Gotch, T.B., 2013. A of artesian springs of the western Great Artesian Basin. In: Lewis, M.M., White, D.C., Gotch, T.B. (Eds.), Allocating Water and Maintaining Springs in the Great Artesian Basin. Vol. IV: Spatial Survey and Remote Sensing of Artesian Springs of the Western Great Artesian Basin. National Water Commission, Canberra.

Love, A.J., Shand, P., Crossey, L., Harrington, G.A., Rousseau-Gueutin, P., 2013. Introduction to groundwater discharge. In: Love, A.J., Shand, P., Crossey, L.,

Harrington, G.A., Rousseau-Gueutin, P. (Eds.), Allocating Water and Maintaining Springs in the Great Artesian Basin. Vol III: Groundwater Discharge of the Western Great Artesian Basin. National Water Commission, Canberra.

Murphy, N.P., Guzik, M.T., Wilmer, J.W., 2010. The influence of landscape on population structure in groundwater springs. Freshwater Biol. 55, 2499–2509.

Petus, C., Lewis, M., White, D., 2013. Monitoring temporal dynamics of Great Artesian Basin wetland vegetation, Australia, using MODIS NDVI. Ecol. Indic. 34, 41–52, http://dx.doi.org/10.1016/j.ecolind.2013.04.009.

Rogers, P.A., Freeman, P.J., 1994. Explanatory notes for the WARRINA 1:250 000 geological map, South Australia, Dept of Mines and Energy.

White, D.C., Gotch, T.B., Alaak, Y., Clark, M., Ryan, J., Lewis, M.M., 2013. Characterising spring groups. In: Lewis, M.M., White, D.C., Gotch, T.B. (Eds.), Allocating Water and Maintaining Springs in the Great Artesian Basin. Vol. IV: Spatial Survey and Remote Sensing of Artesian Springs of the Western Great Artesian Basin. National Water Commission, Canberra.

White, D.C., Lewis, M.M., 2011. A new approach to monitoring spatial distribution and dynamics of wetlands and associated flows of Australian Great Artesian Basin springs using QuickBird satellite imagery. J. Hydrol. 408, 140–152, http://dx.doi.org/10.1016/j.jhydrol.2011.07.032.

White, D.C., Lewis, M.M., 2013. Associating wetland extent and spring flow rates. In: Lewis, M.M., White, D.C., Gotch, T.B. (Eds.), Allocating Water and Maintaining Springs in the Great Artesian Basin. Vol. IV: Spatial Survey and Remote Sensing of Artesian Springs of the Western Great Artesian Basin. National Water Commission, Canberra.

Williams, A.F., Holmes, J.W., 1978. A novel method of estimating the discharge of water from mound springs of the Great Artesian Basin, Central Australia. J. Hydrol. 38, 263–272, http://dx.doi.org/10.1016/0022-1694(78)90073-2.

Wohling, D., Fulton, S., Love, A.J., Dailey, M., Hallihan, T., Berends, V., Purtschert, R., Shand, P., 2013. Mountain system recharge. In: Love, A.J., Wholing, Fulton, S., Rousseau-Gueutin, P., De Ritter, S. (Eds.), Allocating Water and Maintaining Springs in the Great Artesian Basin. Vol II: Groundwater Recharge, Hydrodynamics and Hydrochemistry of the Western Great Artesian Basin. National Water Commission, Canberra.

Wolaver, B., Keppel, M.N., Love, A.J., 2013. Hydrogeology of Dalhousie springs. In: Love, A.J., Shand, P., Crossey, L., Harrington, G.A., Rousseau-Gueutin, P. (Eds.), Allocating Water and Maintaining Springs in the Great Artesian Basin. Vol III: Groundwater Discharge of the Western Great Artesian Basin. National Water Commission, Canberra.